*Note*

# Novel Dammarane-Type Triterpene Saponins from *Panax ginseng* Root

Dong Gu Lee,[a] Ah Young Lee,[b] Kyung-Tack Kim,[c] Eun Ju Cho,[b] and Sanghyun Lee*,[a]

[a] *Department of Integrative Plant Science, Chung-Ang University; Anseong 456–756, Republic of Korea:* [b] *Department of Food Science and Nutrition, Pusan National University; Busan 609–735, Republic of Korea: and* [c] *Korea Food Research Institute; Sungnam 463–746, Republic of Korea.*

Received April 3, 2015; accepted July 27, 2015

**Four phytochemical constituents were isolated from *Panax ginseng* root by repeated column chromatography (CC), medium pressure liquid chromatography (MPLC), high-speed counter current chromatography (HSCCC), and semi-preparative HPLC. Their structures were elucidated as the dammarane-type triterpene saponins ginsenoside-Rg18 (1), 6-acetyl ginsenoside-Rg3 (2), ginsenoside-Rs11 (3), and ginsenoside-Re7 (4) based on spectral data. Compounds 1–4 from *P. ginseng* root were new compounds from nature. They showed good hydroxyl radical scavenging activity and anti-bacterial activity against *Escherichia coli* and *Staphylococcus aureus*. However, they did not show any anti-inflammatory activity. In addition, they inhibited the growth of adenocarcinoma gastric stomach cells. Among them, ginsenoside-Rs11 (3) showed the best anti-oxidative, anti-bacterial, and anti-cancer activities.**

**Key words** *Panax ginseng*; white ginseng; dammarane; ginsenoside-Rs11; adenocarcinoma gastric stomach

*Panax ginseng* (Araliaceae), a traditional oriental herbal medicine, has been used for thousands of years for treating various diseases in East Asian countries.[1,2] *P. ginseng* has attracted significant interest because of its diverse pharmacological and therapeutic effects on the central nervous system, cardiovascular system, and immune-modulating functions. It is used for diabetes, as an anti-oxidant, anti-hypotensive, anti-tumor agent, anti-cancer agent to increase cognitive abilities, as a sedative, and as an analgesic.[3–7] A number of dammarane-type triterpene oligoglycosides with anti-cancer and anti-arrhythmia properties have been reported.[8,9]

The root of ginseng has a critical role in traditional medicine, and its principal constituents have been characterized as dammarane-type triterpene saponins.[10–14] The majority of these compounds are protopanaxadiols (PPD) and protopanaxatriols (PPT), which are aglycones of dammarane-type triterpenes.[15] In PPDs, the sugar moieties are attached to the ring of the triterpene dammarane at the three-position (as in ginsenosides-Rg3, -Rd, -Rc, -Rb1, and -Rb2), while in PPTs, the sugar moieties are attached at the six-position (as in ginsenosides-Rg1, -Re, and -Rg2).[16]

As part of an ongoing study into the chemical and biological activities of ginseng and ginsenosides,[16,17] we describe the isolation, identification, and biological activities of dammarane-type triterpene saponins from the dried root of *P. ginseng*. New compounds were purified by repeated column chromatography (CC), medium pressure liquid chromatography (MPLC), high-speed counter current chromatography (HSCCC), and semi-preparative HPLC (Semiprep-HPLC).

## Results and Discussion

**Identification of Compounds 1–4** The *n*-butanol (*n*-BuOH)-soluble fraction of the ethanol (EtOH) extract from *P. ginseng* root was chromatographed by CC, MPLC, HSCCC, and Semiprep-HPLC to yield compounds **1**–**4** (Fig. 1). Compounds **1**–**4** from *P. ginseng* root were isolated for the first time from nature.

Compound **1** was obtained as a white amorphous powder. The IR spectrum suggested the presence of hydroxyl groups (3365 $cm^{-1}$) and an $\alpha,\beta$-unsaturated carbonyl (1631 $cm^{-1}$). Its UV spectrum in methanol (MeOH) showed absorption maxima at 268, 293, and 394 nm. A molecular ion peak was measured at *m/z* 969 $[M+Na]^+$ in the positive FAB-MS, which corresponds to a molecular formula of $C_{42}H_{72}O_{14}$ by high resolution (HR)-FAB-MS (*m/z* 969.5415 $[M+Na]^+$, Calcd for 969.5399). The $^1$H- and $^{13}$C-NMR data from **1** are shown in Table 1. The $^1$H-NMR spectrum showed one olefinic ($\delta$ 5.26), three anomeric ($\delta$ 5.01, 5.19, and 6.48), and a methyl proton signal ($\delta$ 1.61) of L-rhamnopyranoside. The configuration of the anomeric positions were determined to be the $\alpha$ and $\beta$ form based on the coupling constants for the anomeric proton signals in the $^1$H-NMR spectrum of **1**. In the $^{13}$C-NMR spectrum, the chemical shifts of three anomeric carbons were observed at $\delta$ 98.8, 102.4 and 106.5 with a double bond between C-24 and C-25 ($\delta$ 126.4 and 131.5). Acidic hydrolysis of **1** yielded D-glucopyranoside and L-rhamnopyranoside. Therefore, the anomeric carbon signals indicated two $\beta$-D-glucopyranosyl and one $\alpha$-L-rhamnopyranosyl moieties. The two $\beta$-D-glucopyranosyl anomeric proton signals were confirmed to be linked at the C-6 and C-20 positions by long-range heteronuclear multiple bond connnectivity (HMBC) correlations between the proton signal at $\delta$ 5.01 (H-1′) and the carbon signal at $\delta$ 78.8 (C-6), and the proton signal at $\delta$ 5.19 (H-1″) and the carbon signal at $\delta$ 83.9 (C-20), respectively. A significant downfield shift for the C-2″ ($\delta$ 79.0) was observed for the inner $\beta$-D-glucopyranosyl moiety at C-20 of the aglycone, which showed that the C-1‴ ($\delta$ 6.48) in the terminal $\alpha$-L-rhamnopyranosyl moiety is linked to the inner $\beta$-D-glucopyranosyl moiety at C-20.[18] Based on this data, the structure of **1** was identified as ginsenoside-Rg18.

Compound **2** was obtained as a white amorphous powder. Its IR spectrum suggested the presence of hydroxyl groups (3365 $cm^{-1}$) and an $\alpha,\beta$-unsaturated carbonyl (1631 $cm^{-1}$). Its UV spectrum in MeOH showed absorption maxima at 268, 293, and 394 nm. A molecular ion peak was measured at *m/z* 1027 $[M+Na]^+$ in the positive FAB-MS, which corre-

* To whom correspondence should be addressed. e-mail: slee@cau.ac.kr

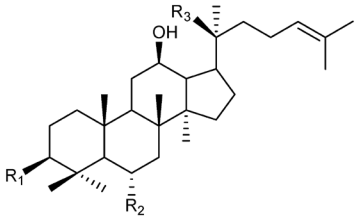


**1** $R_1$: -OH $R_2$: -OGlc $R_3$: -OGlc(2→1)ORha

**2** $R_1$: -OH $R_2$: -OGlc(4→1)OGlc $R_3$: -OGlc(6)OAc

**3** $R_1$: -OGlc(2→1)OGlc(6)OAc $R_2$: -H $R_3$: -OGlc(6→1)OAra(f)

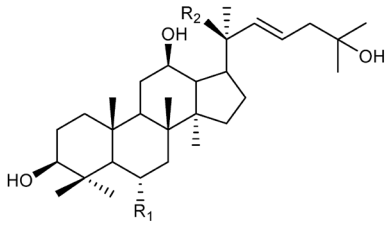


**4** $R_1$: -OGlc(2→1)ORha $R_2$: -OGlc

Fig. 1. Structures of Compounds **1**–**4**

sponds to a molecular formula of $C_{50}H_{84}O_{20}$ by HR-FAB-MS (*m/z* 1143.2217 $[M+Na]^+$, Calcd for 1143.2220). The $^1$H- and $^{13}$C-NMR data of **2** are shown in Table 1. The $^1$H-NMR spectrum showed one olefinic ($\delta$ 5.30), three anomeric ($\delta$ 5.00, 5.01, and 5.18), and an acetyl methyl proton signal ($\delta$ 2.05). The configuration of the anomeric positions were determined to be the $\beta$ form based on the coupling constants of the anomeric proton signals in the $^1$H-NMR spectrum of **2**. In the $^{13}$C-NMR spectrum, the chemical shifts of three anomeric carbons were observed at $\delta$ 98.8, 106.3, and 106.4. Acidic hydrolysis of **2** yielded D-glucopyranoside. Therefore, the anomeric carbon signals indicated three $\beta$-D-glucopyranosyl moieties. The two $\beta$-D-glucopyranosyl anomeric proton signals were confirmed to be linked at the C-6 and C-20 positions by long-range HMBC correlations between the proton signal at $\delta$ 5.00 (H-1′) and carbon signal at $\delta$ 79.3 (C-6), and the proton signal at $\delta$ 5.18 (H-1‴) and carbon signal at $\delta$ 83.9 (C-20), respectively. A significant downfield shift for the C-4′ ($\delta$ 76.0) was observed for the inner $\beta$-D-glucopyranosyl moiety at C-6 of the aglycone, which showed that the C-1″ ($\delta$ 5.01) in the terminal $\beta$-D-glucopyranosyl moiety is linked to the inner $\beta$-D-glucopyranosyl moiety at C-6. In the $^1$H-NMR spectrum of **2**, the downfield shift of two hydroxymethylene proton signals ($\delta$ 5.05 and 4.62) was attributed to acetylation of the hydroxyl group. These signals also showed a correlation with C-5‴ ($\delta$ 75.9), thus the acetyl group was placed at the primary hydroxyl group of the sugar moiety (C-6‴). The NMR assignments of compound **2** were very similar to 6-acetyl-Rg1, previously isolated from red ginseng, except for the position of the $\beta$-D-glucopyranosyl group at the C-4′ hydroxyl of the sugar moiety.[19] Based on this data, the structure of **2** was identified as 6-acetyl ginsenoside-Rg3.

Compound **3** was isolated as a white amorphous powder. The IR spectrum suggested the presence of hydroxyl groups (3365 $cm^{-1}$) and an $\alpha,\beta$-unsaturated carbonyl (1631 $cm^{-1}$). Its UV spectrum in MeOH showed absorption maxima at 268, 293, and 394 nm. A molecular ion peak was measured at *m/z* 1,143 $[M+Na]^+$ in the positive FAB-MS, which corresponds to a molecular formula of $C_{55}H_{92}O_{23}$ by HR-FAB-MS (*m/z* 1143.5922 $[M+Na]^+$, Calcd for 1143.5927). The $^1$H- and $^{13}$C-NMR data from **3** are shown in Table 1. The $^1$H-NMR spectrum showed one olefinic ($\delta$ 5.44), four anomeric ($\delta$ 4.93, 5.21, 5.40 and 5.67), and an acetyl methyl proton signal ($\delta$ 2.06). The configuration of the anomeric positions were determined to be the $\alpha$ and $\beta$ form based on the coupling constants of the anomeric proton signals in the $^1$H-NMR spectrum of **3**. In the $^{13}$C-NMR spectrum, the chemical shifts of four anomeric carbons were observed at $\delta$ 98.8, 105.6, 106.8, and 110.6. Acidic hydrolysis of **3** afforded D-glucopyranoside and L-arabinofuranoside. Therefore, the anomeric carbon signals indicated three $\beta$-D-glucopyranosyl and one $\alpha$-L-arabinofuranosyl moieties. A significant downfield shift for the C-2′ ($\delta$ 83.9) was observed for the inner $\beta$-D-glucopyranosyl moiety at C-3 of the aglycone, which showed that the terminal $\beta$-D-glucopyranosyl moiety is linked to the inner $\beta$-D-glucopyranosyl moiety at C-3. In the $^1$H-NMR spectrum of **3**, the downfield shift of two hydroxymethylene proton signals ($\delta$ 4.94 and 4.81) was attributed to acetylation of the hydroxyl group. These two proton signals were confirmed to be linked at the C-4′ and C-2′ positions by long-range HMBC correlations between the proton signal at $\delta$ 4.94 (H-6″$\alpha$) and the carbon signal at $\delta$ 72.1 (C-4′), and the proton signal at $\delta$ 4.81 (H-6″$\beta$) and the carbon signal at $\delta$ 83.9 (C-2′), respectively. Therefore, the acetyl was placed at the primary hydroxyl group of the sugar moiety (C-6″). The NMR assignments of compound **3** were very similar to those of ginsenoside Rs2, previously isolated from red ginseng, except for the position of the acetyl group at the C-6″ hydroxyl of the sugar moi-

Table 1. $^{1}$H- and $^{13}$C-NMR Data for the Agylcone and Sugar Moieties of Compounds **1**–**4** (500 MHz, Pyridine-$d_5$)

| No. | **1** | | **2** | | **3** | | **4** | |
|---|---|---|---|---|---|---|---|---|
| | $\delta_H$ | $\delta_C$ | $\delta_H$ | $\delta_C$ | $\delta_H$ | $\delta_C$ | $\delta_H$ | $\delta_C$ |
| 1 | 0.74, 1.51 | 39.9 | 0.81, 1.54 | 40.0 | 0.82, 1.45 | 39.7 | 0.75, 1.50 | 40.0 |
| 2 | 1.81, 2.15 | 28.4 | 1.82, 2.19 | 28.3 | 1.79, 1.97 | 28.6 | 1.75, 2.03 | 28.3 |
| 3 | 3.52 | 79.8 | 3.54 | 80.7 | 3.49 | 89.5 | 3.48 | 80.1 |
| 4 | — | 41.6 | — | 40.3 | — | 40.2 | — | 39.9 |
| 5 | 1.45 | 61.9 | 1.51 | 62.0 | 1.49 | 56.9 | 1.45 | 61.4 |
| 6 | 4.63 | 78.8 | 4.63 | 79.3 | 4.37 | 18.9 | 4.35 | 76.3 |
| 7 | 1.95, 2.54 | 45.6 | 1.84, 2.46 | 46.0 | 1.88, 2.45 | 35.7 | 1.78, 2.51 | 46.3 |
| 8 | — | 41.7 | — | 40.8 | — | 40.5 | — | 40.8 |
| 9 | 1.56 | 51.9 | 1.52 | 49.7 | 1.53 | 49.9 | 1.57 | 49.5 |
| 10 | — | 39.9 | — | 41.7 | — | 37.4 | | 40.5 |
| 11 | 1.41, 1.95 | 31.4 | 1.43, 1.87 | 32.1 | 1.50, 2.09 | 31.2 | 1.45, 1.93 | 31.1 |
| 12 | 3.95 | 70.8 | 4.03 | 70.9 | 3.90 | 70.7 | 4.01 | 70.1 |
| 13 | 1.99 | 50.5 | 1.95 | 52.0 | 2.06 | 50.7 | 2.02 | 50.0 |
| 14 | — | 51.9 | — | 52.2 | — | 51.9 | — | 52.2 |
| 15 | 1.16, 1.72 | 31.4 | 1.02, 1.67 | 31.4 | 0.97, 1.52 | 31.4 | 1.15, 1.65 | 31.1 |
| 16 | 1.42, 1.85 | 23.8 | 1.35, 1.85 | 23.9 | 1.32, 1.77 | 23.7 | 1.37, 1.84 | 23.3 |
| 17 | 2.45 | 52.2 | 2.54 | 50.5 | 2.36 | 52.3 | 2.42 | 50.5 |
| 18 | 1.05 | 18.3 | 0.94 | 18.4 | 0.94 | 16.4 | 1.15 | 18.1 |
| 19 | 0.92 | 18.1 | 1.02 | 18.1 | 1.04 | 16.7 | 0.98 | 18.0 |
| 20 | — | 83.9 | — | 83.9 | — | 83.9 | — | 83.7 |
| 21 | 1.58 | 19.3 | 1.54 | 18.1 | 1.52 | 17.8 | 1.51 | 18.3 |
| 22 | 1.79, 2.33 | 36.5 | 2.08, 2.71 | 36.6 | 1.83, 2.27 | 36.6 | 5.70 | 127.0 |
| 23 | 2.24, 2.51 | 22.9 | 3.08, 3.45 | 23.1 | 2.45, 2.75 | 22.9 | 6.16 | 138.7 |
| 24 | 5.26 | 126.4 | — | 126.5 | 5.44 | 126.5 | 2.22, 2.54 | 39.8 |
| 25 | — | 131.5 | — | 131.6 | — | 131.5 | — | 81.9 |
| 26 | 1.59 | 26.2 | 5.74, 6.31 | 26.3 | 1.55 | 26.3 | 1.57 | 25.8 |
| 27 | 1.55 | 18.0 | 1.86 | 18.1 | 1.52 | 18.2 | 1.60 | 25.9 |
| 28 | 2.10 | 32.2 | 2.12 | 32.3 | 1.25 | 28.6 | 2.15 | 33.3 |
| 29 | 1.64 | 18.2 | 1.57 | 17.1 | 1.11 | 17.1 | 1.35 | 17.7 |
| 30 | 0.87 | 18.2 | 0.91 | 17.7 | 0.94 | 16.9 | 0.82 | 17.7 |
| COCH3 | — | — | — | 171.6 | — | 171.6 | — | — |
| COCH3 | — | — | 2.05 | 21.5 | 2.06 | 21.4 | — | — |
| 3-O-glc-1′ | — | — | — | — | 4.93 | 105.6 | — | — |
| 2′ | — | — | — | — | 4.17 | 83.9 | — | — |
| 3′ | — | — | — | — | 4.23 | 78.8 | — | — |
| 4′ | — | — | — | — | 3.99 | 72.1 | — | — |
| 5′ | — | — | — | — | 4.09 | 75.6 | — | — |
| 6′ | — | — | — | — | 4.94, 4.81 | 65.3 | — | — |
| 2′-O-glc-1″ | — | — | — | — | 5.40 | 106.8 | — | — |
| 2″ | — | — | — | — | 4.15 | 77.6 | — | — |
| 3″ | — | — | — | — | 4.17 | 78.6 | — | — |
| 4″ | — | — | — | — | 4.31 | 72.2 | — | — |
| 5″ | — | — | — | — | 4.01 | 79.7 | — | — |
| 6″ | — | — | — | — | 4.49, 4.23 | 63.3 | — | — |
| 6-O-glc-1′ | 5.01 | 106.5 | 5.00 | 106.3 | — | — | 5.25 | 102.4 |
| 2′ | 4.10 | 75.7 | 4.11 | 75.6 | — | — | 4.00 | 79.8 |
| 3′ | 4.22 | 78.8 | 4.21 | 78.8 | — | — | 4.21 | 79.7 |
| 4′ | 4.24 | 72.4 | 4.25 | 76.0 | — | — | 4.18 | 71.9 |
| 5′ | 4.01 | 78.6 | 4.02 | 78.6 | — | — | 3.98 | 78.6 |
| 6′ | 4.50, 4.34 | 63.6 | 4.35, 4.23 | 63.3 | — | — | 4.50, 4.38 | 63.6 |
| 2′-O-rha-1″ | — | — | — | — | — | — | 6.49 | 102.4 |
| 2″ | — | — | — | — | — | — | 4.51 | 72.8 |
| 3″ | — | — | — | — | — | — | 4.67 | 72.9 |
| 4″ | — | — | — | — | — | — | 4.22 | 74.7 |
| 5″ | — | — | — | — | — | — | 4.93 | 70.5 |
| 6″ | | | — | — | — | — | 1.77 | 19.2 |
| 2′-O-glc-1″ | — | — | 5.01 | 106.4 | — | — | — | — |
| 2″ | — | — | 4.19 | 75.6 | — | — | — | — |

Table 1. Continued

| No. | 1 | | 2 | | 3 | | 4 | |
|---|---|---|---|---|---|---|---|---|
| | $\delta_H$ | $\delta_C$ | $\delta_H$ | $\delta_C$ | $\delta_H$ | $\delta_C$ | $\delta_H$ | $\delta_C$ |
| 3″ | — | — | 4.49 | 79.3 | — | — | — | — |
| 4″ | — | — | 4.11 | 72.4 | — | — | — | — |
| 5″ | — | — | 3.99 | 78.8 | — | — | — | — |
| 6″ | — | — | 4.49, 4.27 | 63.6 | — | — | — | — |
| 20-O-glc-1″ | 5.19 | 98.8 | — | — | — | — | — | — |
| 2″ | 3.99 | 79.0 | — | — | — | — | — | — |
| 3″ | 4.20 | 79.6 | — | — | — | — | — | — |
| 4″ | 4.20 | 72.0 | — | — | — | — | — | — |
| 5″ | 4.00 | 76.0 | — | — | — | — | — | — |
| 6″ | 4.37, 4.21 | 63.3 | — | — | — | — | — | — |
| 20-O-glc-1‴ | — | — | 5.18 | 98.8 | 5.21 | 98.8 | 5.19 | 98.8 |
| 2‴ | — | — | 4.08 | 75.7 | 3.98 | 75.6 | 3.98 | 74.7 |
| 3‴ | — | — | 4.20 | 79.7 | 4.19 | 78.7 | 4.22 | 79.2 |
| 4‴ | — | — | 4.23 | 72.0 | 4.22 | 72.6 | 4.20 | 72.1 |
| 5‴ | — | — | 4.05 | 75.9 | 4.09 | 78.8 | 3.97 | 78.8 |
| 6‴ | — | — | 5.05, 4.62 | 65.8 | 4.29, 4.19 | 69.0 | 4.36, 4.23 | 63.4 |
| 2″-O-rha-1⁗ | 6.48 | 102.4 | — | — | — | — | — | — |
| 2⁗ | 4.50 | 72.8 | — | — | — | — | — | — |
| 3⁗ | 4.37 | 73.1 | — | — | — | — | — | — |
| 4⁗ | 4.33 | 74.7 | — | — | — | — | — | — |
| 5⁗ | 4.35 | 70.1 | — | — | — | — | — | — |
| 6⁗ | 1.61 | 19.3 | | | — | — | — | — |
| 6‴-O-ara(f)-1⁗ | — | — | — | — | 5.67 | 110.6 | — | — |
| 2⁗ | — | — | — | — | 4.21 | 84.8 | — | — |
| 3⁗ | — | — | — | — | 4.78 | 79.7 | — | — |
| 4⁗ | — | — | — | — | 4.78 | 86.5 | — | — |
| 5⁗ | — | — | — | — | 4.22, 4.46 | 63.2 | — | — |

Chemical shifts are reported in parts per million ($\delta$).

ety.[20,21] Based on this data, the structure of **3** was identified as ginsenoside-Rs11.

Compound **4** was obtained as a white amorphous powder. The IR spectrum suggested the presence of hydroxyl groups (3365 $cm^{-1}$) and an $\alpha,\beta$-unsaturated carbonyl (1631 $cm^{-1}$). Its UV spectrum in MeOH showed absorption maxima at 268, 293, and 394 nm. A molecular ion peak was measured at *m/z* 985 $[M+Na]^+$ in the positive FAB-MS, which corresponds to a molecular formula of $C_{48}H_{82}O_{19}$ by HR-FAB-MS (*m/z* 985.5373 $[M+Na]^+$, Calcd for 985.5348). The $^1$H- and $^{13}$C-NMR data from **4** are shown in Table 1. The $^1$H-NMR spectrum showed two olefinic ($\delta$ 6.16 and 6.26), three anomeric ($\delta$ 5.19, 5.25, and 6.49), and a methyl proton signal ($\delta$ 1.77) of L-rhamnopyranoside. The configuration of the anomeric positions were determined to be the $\alpha$ and $\beta$ form based on the coupling constants of the anomeric proton signals in the $^1$H-NMR spectrum of **4**. In the $^{13}$C-NMR spectrum, the chemical shifts of three anomeric carbons were observed at $\delta$ 98.8, 102.4, and 102.4 (overlap). In the HMBC spectrum, correlations were observed between the proton signal at $\delta$ 5.70 (H-22) and the carbon signals at $\delta$ 40.2 (C-24) and 81.9 (C-25), and the proton signal at $\delta$ 6.26 (H-23) and the carbon signals at $\delta$ 40.2 (C-24), 81.9 (C-25), 25.8 (C-26), and 25.9 (C-27), respectively. Up to this point it could be concluded that the double bond might be located between C-22 and C-23.[22,23] Acidic hydrolysis of **4** yielded D-glucopyranoside and L-rhamnopyranoside. Therefore, the anomeric carbon signals indicated two $\beta$-D-glucopyranosyl and one $\alpha$-L-rhamnopyranosyl moieties. The two $\beta$-D-glucopyranosyl anomeric proton signals were confirmed to be linked at the C-6 and C-20 positions by long-range HMBC correlations between the proton signal at $\delta$ 5.25 (H-1′) and carbon signal at $\delta$ 80.1 (C-6), and the proton signal at $\delta$ 5.19 (H-1‴) and the carbon signal at $\delta$ 83.7 (C-20), respectively. A significant downfield shift for the C-2′ ($\delta$ 79.8) was observed for the inner $\beta$-D-glucopyranosyl moiety at C-6 of the aglycone, which showed that the C-1″ ($\delta$ 6.49) of the terminal $\alpha$-L-rhamnopyranosyl moiety is linked to the inner $\beta$-D-glucopyranosyl moiety at C-6. Based on this data, the structure of **4** was identified as ginsenoside-Re7.

**Biological Activities of Compounds 1–4** The 1,1-diphenyl-2-picrylhydrazyl (DPPH) radical contains an odd electron that is responsible for its absorbance at 540 nm, and for the visible deep purple color. A higher % in our assay indicates better scavenging activity or anti-oxidant potential. As shown in Table 2, ginsenoside-Rg18 (**1**), 6-acetyl ginsenoside-Rg3 (**2**), ginsenoside-Rs11 (**3**), and ginsenoside-Re7 (**4**) had weak DPPH radical-scavenging activity. The ·OH scavenging activity of ginsenoside-Rg18 (**1**), 6-acetyl ginsenoside-Rg3 (**2**), ginsenoside-Rs11 (**3**), and ginsenoside-Re7 (**4**) was greater than 85% at a concentration of 50 $\mu$M. Ginsenoside-Rs11 (**3**) in particular had a scavenging activity of greater than 90% under the same conditions. These results suggest that ginsenoside-Rs11 (**3**) may be an effective scavenger of ·OH radicals.

The anti-bacterial activities of ginsenoside-Rg18 (**1**), 6-acetyl ginsenoside-Rg3 (**2**), ginsenoside-Rs11 (**3**), and ginsenoside-Re7 (**4**) against *Escherichia* (*E.*) *coli*, *Staphylo-*

Table 2. Anti-oxidative Activities of Compounds **1–4**

| Sample | Radical scavenging activity (%) | | |
|---|---|---|---|
| | Concentration ($\mu$M) | DPPH | ·OH |
| **1** | 50 | 8.76±1.03[a] | 87.70±0.26[c] |
| | 10 | 5.18±0.65[cd] | 85.71±0.10[f] |
| **2** | 50 | 4.58±0.76[d] | 87.55±0.21[cd] |
| | 10 | 2.39±1.03[e] | 87.18±0.43[d] |
| **3** | 50 | 7.37±0.76[ab] | 90.74±0.20[a] |
| | 10 | 6.37±0.80[bc] | 86.24±0.20[d] |
| **4** | 50 | 2.19±0.40[e] | 89.48±0.20[b] |
| | 10 | 2.39±0.46[e] | 84.67±0.31[g] |
| L-Ascorbic acid* ($IC_{50}$, $\mu$M) | | 5.77±0.07 | 0.24±0.01 |

*L-Ascorbic acid was used as a positive control. Values are the mean±S.D. [a–g]Means with different letters are significantly different ($p<0.05$) by Duncan's multiple range test.

Table 3. Anti-bacterial Activities of Compounds **1–4**

| Sample (500 $\mu$M) | Clear zone (mm) | | |
|---|---|---|---|
| | *E. coli* | *S. aureus* | *H. pylori* |
| **1** | 10 | 13 | — |
| **2** | 11 | 12 | — |
| **3** | 14 | 12 | — |
| **4** | 12 | 12 | — |

*coccus* (*S.*) *aureus*, and *Helicobacter* (*H.*) *pylori* are shown in Table 3. Ginsenoside-Rg18 (**1**), 6-acetyl ginsenoside-Rg3 (**2**), ginsenoside-Rs11 (**3**), and ginsenoside-Re7 (**4**) inhibited the growth of *E. coli* and *S. aureus* at a concentration of 500 $\mu$M. In particular, ginsenoside-Rs11 (**3**) showed good antibacterial activity against *E. coli*.

The anti-inflammatory activity was investigated using RAW264.7 cells stimulated by lipopolysaccharide (LPS)/interferon (IFN)-$\gamma$. As shown in Table 4, there was no significant difference in cell viability between the normal group and the control group, which were measured at approximately 100 and 99.74%, respectively. RAW264.7 cells were incubated with the inflammatory mediators LPS and IFN-$\gamma$, which induced the generation of nitric oxide (NO). Secretion of NO from RAW264.7 macrophage cells in the normal group decreased 52.91% compared to the control group (100%). Treatment of the RAW264.7 cells with ginsenoside-Rg18 (**1**), 6-acetyl ginsenoside-Rg3 (**2**), ginsenoside-Rs11 (**3**), and ginsenoside-Re7 (**4**) did not lead to a decrease in NO production (Table 4). This result indicates that the saponins did not show anti-inflammatory activity.

To assess the cytotoxic activity, we used the 3-(4,5-dimethylthiazol-2-yl)-2,5-diphenyltetrazolium bromide (MTT) method to test whether these extracts moderated the growth of adenocarcinoma gastric stomach (AGS) cells. Cell viability was measured by detecting the purple formazan metabolized in MTT by mitochondrial dehydrogenases, which are active only in live cells. Cells were incubated for 1 d and then treated with ginsenoside-Rg18 (**1**), 6-acetyl ginsenoside-Rg3 (**2**), ginsenoside-Rs11 (**3**), and ginsenoside-Re7 (**4**) at 50 $\mu$M, which all caused some inhibition of gastric cancer cell growth. In particular, ginsenoside-Rs11 (**3**) had the greatest

Table 4. Cell Viability and NO Production of Compounds **1–4** in RAW 264.7 Cells Treated with LPS/IFN-$\gamma$

| Sample | Concentration ($\mu$M) | Cell viability (%) | NO generation (%) |
|---|---|---|---|
| **1** | 50 | 93.18±1.36[bc] | 99.09±1.06[bc] |
| | 10 | 88.48±0.56[e] | 97.55±0.33[c] |
| **2** | 50 | 90.36±1.19[d] | 98.69±0.56[bc] |
| | 10 | 90.80±1.89[cd] | 99.20±0.85[bc] |
| **3** | 50 | 88.08±0.87[e] | 98.27±1.31[bc] |
| | 10 | 90.90±0.40[cd] | 98.76±0.96[bc] |
| **4** | 50 | 92.04±1.17[bc] | 103.19±0.86[a] |
| | 10 | 90.99±0.60[cd] | 101.67±1.51[a] |
| Normal | | 100.00±0.32[a] | 52.91±0.49[b] |
| Control | | 99.74±0.95[a] | 100.00±0.64[d] |
| AMT* | | 91.49±1.17 | 40.59±1.15 |

*AMT was used as a positive control. Values are the mean±S.D. [a–d]Means with different letters are significantly different ($p<0.05$) by Duncan's multiple range test.

Table 5. Cytotoxic Activities of Compounds **1–4**

| Sample | Concentration ($\mu$M) | AGS cell growth inhibition rate (%) |
|---|---|---|
| **1** | 50 | 38.01±0.41[b] |
| | 10 | 37.29±5.36[b] |
| **2** | 50 | 44.12±7.35[ab] |
| | 10 | 37.36±8.24[b] |
| **3** | 50 | 55.06±3.97[a] |
| | 10 | 46.53±4.97[ab] |
| **4** | 50 | 51.06±9.75[a] |
| | 10 | 43.65±5.49[ab] |
| 5-Fluorouracil* | 50 | 45.47±0.50 |

*5-Fluorouracil (10 $\mu$M) was used as a positive control. Values are the mean±S.D. [a–b]Means with different letters are significantly different ($p<0.05$) by Duncan's multiple range test.

cancer cell growth inhibition (55.06%) of the various extracts. Ginsenoside-Rg18 (**1**) had the smallest effect, inhibiting the AGS cell growth rate by 38.01%. These experiments show that ginsenoside-Rg18 (**1**), 6-acetyl ginsenoside-Rg3 (**2**), ginsenoside-Rs11 (**3**), and ginsenoside-Re7 (**4**) have a significant anti-proliferative effect on AGS cells (Table 5).

As part of an ongoing study into the chemical and biological activities of ginseng and ginsenosides, we describe the isolation, identification, and biological activities of dammarane-type triterpene saponins from the dried root of *P. ginseng*. These results will be beneficial for the application of ginsenosides from *P. ginseng* in the nutraceutical, pharmaceutical, and cosmeceutical areas.

## Experimental

**Plant Materials** *P. ginseng* C. A. MEYER was collected from Geumsan, Chungcheong Province, Republic of Korea in 2010. The collected root was dried and powdered by Korea Food Research Institute, Sungnam 463–746, Republic of Korea.

**Apparatus and Chemicals** Solvents including analytical grade of EtOH, *n*-hexane, chloroform ($CHCl_3$), ethyl acetate (EtOAc), and *n*-BuOH (SamChun Pure Chemical Co., Pyeongtaek, Republic of Korea) were used as mobile phase for MPLC. Acetonitrile (ACN) and water (HPLC-grade) were purchased from J. T. Baker (Phillipsburg, NJ, U.S.A.). Pyridine-$d_5$ (Milford, MA, U.S.A.) was used as an NMR

solvent. Optical rotations were measured on a Jasco P-2000 digital polarimeter. Fast atom bombardment (FAB) MS was performed with a Jeol JMS-AX505WA mass spectrometer. $^{1}$H- and $^{13}$C-NMR spectra were recorded with a Bruker AVANCE 500 NMR spectrometer (Bremen, Germany) using tetramethylsilane (TMS) as the internal standard. Chemical shifts are reported in parts per million ($\delta$), and coupling constants ($J$) are expressed in Hz. An Eyela rotary evaporator system (Tokyo, Japan) was used for *in vacuo* evaporation. TLC was performed on Kiesel gel 60 $F_{254}$ (250 $\mu$m) silica gel plate (Art. 5715, Merck Co., Darmstadt, Germany), and visualized by spraying a 10% $H_2SO_4$ in MeOH solution, followed by heating to 100°C. CC was conducted with a LiChroprep RP-18 (40–63 $\mu$m, Merck Co., Germany). An MPLC system (Biotage, Uppsala, Sweden) equipped with cartridges (KP-SIL, 39×225 mm) was used. A HSCCC system (Tauto Biotech Co., Ltd., Shanghai, China) was equipped with three preparative coils (i.d. 1.5 mm, total volume is 300 mL, and a 20 mL sample loop). HPLC chromatograms were recorded on a Waters 1525 Binary HPLC Pump (Milford) equipped with a Waters 2489 UV/Vis detector (Milford). Semiprep-HPLC was carried out on an Agilent series 1260 separation system (Santa Clara, CA, U.S.A.) with a fraction collector, a 1260 Quat pump VL, and a 1260 Variable Wavelength Detector. Samples were separated using an Eclipse XDB-$C_{18}$ Semiprep column (5 $\mu$m, 9.4×150 mm) at a flow rate of 1.0 mL/min. Sugar determinations were carried out with a HP 5890 series II GC (Hewlett-Packard, Avondale, PA, U.S.A.) using a DB-1 capillary column (30 m×0.25 mm i.d., Agilent, J&W Scientific, Folsom, CA, U.S.A.) [column temperature: 230°C; detector temperature: 200°C; injector temperature: 200°C; He gas flow rate: 1 mL/min]. The 1,1-diphenyl-2-picrylhydrazyl (DPPH) and 2-deoxyribose used to investigate radical-scavenging activity were obtained from Sigma Chemical Co. (MO, U.S.A.), and hydrogen peroxide ($H_2O_2$) was purchased from Junsei Chemical Co. (Tokyo, Japan). AGS and RAW264.7 cells were obtained from the Korea Cell Line Bank (KCLB, Seoul, Korea). Dulbecco's modified Eagle's medium (DMEM), Roswell Park Memorial Institute 1640 (RPMI-1640), fetal bovine serum (FBS), and penicillin/streptomycin were obtained from Welgene (Daegu, Republic of Korea). The lipopolysaccharide (LPS) used in this study was from Sigma Chemical Co. (MO, U.S.A.), and interferon-gamma (IFN-$\gamma$) was from Pepro Tech (NJ, U.S.A.). The Griess reagent, MTT, 3,3-tetramethylene glutaric acid (TMG), and dimethyl sulfoxide (DMSO) were obtained from Sigma Chemical Co.

**Extraction and Isolation** The dried and powdered root of *P. ginseng* (7.0 kg) was extracted with EtOH (3×21 L), heated to reflux, and the extracts were combined and concentrated to afford a brown residue (139 g). The residue was dissolved in water (7 L) and partitioned successively with *n*-hexane (3×7 L), $CHCl_3$ (3×7 L), EtOAc (3×7 L), and *n*-BuOH (3×7 L) to give the *n*-hexane-soluble (50 g), chloroform ($CHCl_3$)-soluble (11 g), EtOAc-soluble (11 g), and *n*-BuOH-soluble (50 g) fractions. The *n*-BuOH extract (50 g) was separated by MPLC using $CHCl_3$–MeOH as the mobile phase (gradient: 100 : 0→0 : 100, v/v). Thirteen fractions were obtained by combing those with similar *Rf* on TLC behavior (1→13). Fraction 4 (8 g, $V_e/V_t$=0.15) was repeatedly chromatographed by MPLC using $CHCl_3$–MeOH (gradient: 100 : 0→0 : 100, v/v) as the mobile phase (total volume=1254 mL) to obtain 7 fractions (WGB 4.1–4.7). The combined fractions (WGB 4.5, 4.6 and 4.7; 3 g, $V_e/V_t$=0.42) were separated by MPLC using $CHCl_3$–MeOH (gradient: 90 : 10→0 : 100, v/v) as the mobile phase (total volume=748 mL) to obtain 6 fractions (WGB 4.5.1–4.5.6). WGB 4.5.2 (920 mg, $V_e/V_t$=0.12) was separated by MPLC using $CHCl_3$–MeOH (gradient: 75 : 25→100 : 0, v/v) as the mobile phase (total volume=2948 mL) to obtain 6 fractions (WGB 4.5.2.1–4.5.2.6). WGB 4.5.2.4 (320 mg, $V_e/V_t$=0.09) was separated on a LiChroprep RP18 column ($\phi$1.0×32 cm) using MeOH–water (gradient: 1 : 3→1 : 0, v/v) as the mobile phase (total volume=400 mL) to obtain 3 fractions (WGB 4.5.2.4.1–4.5.2.4.3). WGB 4.5.2.4.2 (290 mg, $V_e/V_t$=0.1) was separated by HSCCC using EtOAc–*n*-BuOH–water (4 : 1 : 6; v/v/v; 850 rpm, 1 mL/min) as the mobile phase to afford 3 additional fractions (WGB 4.5.2.4.2.1–4.5.2.4.2.3). WGB 4.5.2.4.2.3 was further separated by Semiprep-HPLC using ACN/water (gradient: 20 : 80→0 : 100, v/v) as the mobile phase to afford 5 additional fractions (WGB 4.5.2.4.2.3.1–4.5.2.4.2.3.5) including compound **1** (65 mg, WGB 4.5.2.4.2.3.3). Fraction 5 (8 g, $V_e/V_t$=0.17) was repeatedly chromatographed by MPLC using $CHCl_3$–MeOH (gradient: 100 : 0→0 : 100, v/v) as the mobile phase (total volume=1932 mL) to obtain 9 fractions (WGB 5.1–5.9). WGB 5.5 (120 mg, $V_e/V_t$=0.07) was separated by MPLC using $CHCl_3$–MeOH (gradient: 100 : 0→0 : 100, v/v) as the mobile phase (total volume=882 mL) to obtain 5 fractions (WGB 5.5.1–5.5.5). WGB 5.5.2 (10 mg, $V_e/V_t$=0.10) was separated with a LiChroprep RP18 column ($\phi$1.0×32 cm) using MeOH–water (gradient: 1 : 3→1 : 0, v/v) as the mobile phase (total volime=400 mL) to obtain 10 fractions (WGB 5.5.2.1–5.5.2.10) including compound **2** (27 mg, WGB 5.5.2.5). WGB 5.8 (320 mg, $V_e/V_t$=0.11) was separated by MPLC using $CHCl_3$–MeOH (gradient: 80 : 20→0 : 100, v/v) as the mobile phase (total volume=3600 mL) to obtain 7 fractions (WGB 5.8.1–5.8.7). WGB 5.8.5 (55 mg, $V_e/V_t$=0.02) was separated by MPLC using $CHCl_3$–MeOH (gradient: 80 : 20→0 : 100, v/v) as the mobile phase (total volume=2,100 mL) to obtain 10 fractions (WGB 5.8.5.1–5.8.5.10). WGB 5.8.5.3 (10 mg, $V_e/V_t$=0.08) was separated with a LiChroprep RP18 column ($\phi$1.0×32 cm) using MeOH–water (gradient: 1 : 3→1 : 0, v/v) as the mobile phase (total volume=500 mL) to obtain 10 fractions (WGB 5.8.5.3.1–5.8.5.3.10) including compound **3** (26.5 mg, WGB 5.8.5.3.8). WGB 5.8.6 (61 mg, $V_e/V_t$=0.02) was separated by MPLC using $CHCl_3$–MeOH (gradient: 80 : 20→0 : 100, v/v) as the mobile phase (total volume=2100 mL) to obtain 10 fractions (WGB 5.8.6.1–5.8.6.10). WGB 5.8.6.4 (40 mg, $V_e/V_t$=0.03) was separated with a LiChroprep RP18 column ($\phi$1.0×32 cm) using MeOH–water (gradient: 1 : 3→1 : 0, v/v) as the mobile phase (total volume=680 mL) to obtain 7 fractions (WGB 5.8.6.4.1–5.8.6.4.7). WGB 5.8.6.4.2 (21 mg, $V_e/V_t$=0.09) was further separated by Semiprep-HPLC using ACN–water (gradient: 20 : 80→0 : 100, v/v) to afford 6 additional fractions (WGB 5.8.6.4.2.1–5.8.6.4.2.6) including compound **4** (33 mg, WGB 5.8.6.4.2.1).

**Acidic Hydrolysis of Compounds 1–4** Compounds **1**–**4** (each 10 mg) were heated to reflux in a mixture of 5% HCl in 60% aqueous dioxane (10 mL) for 2 h. The reaction mixture was concentrated under reduced pressure, and the residue was extracted with ether. The ether extract was concentrated to afford aglycone hederagenin, which was identified by direct comparison with an authentic sample. The water layer was neutralized with $Ag_2CO_3$, the remaining solid was removed

by filtration, and the filtrate was concentrated under reduced pressure. The residue was compared with standard sugars by cellulose TLC (pyridine–EtOAc–HOAc–water, 36 : 36 : 7 : 21, v/v/v/v), and the sugars were identified as L-rhamnopyranoside and D-glucopyranoside.

**Determination of the Absolute Configuration of Sugars in Compounds 1–4** Compounds **1–4** (each 10 mg) were treated as previously described. The dried sugar mixture was dissolved in pyridine (0.1 mL), and added to a pyridine solution (0.1 mL) of L-cysteine methyl ester hydrochloride (2 mg) followed by warming to 60°C for 1 h. The solvent was evaporated under a $N_2$ stream and the residue was dried *in vacuo*. The residue was trimethylsilylated with TMS-HT (0.1 mL) at 60°C for 30 min. After addition of *n*-hexane and water to the trimethylsilylated residue, the *n*-hexane layer was separated and analyzed by GC. The retention times ($t_R$) of the peaks were 5.58 (L-arabinofuranoside), 6.18 (L-rhamnopyranoside), and 22.03 min (D-glucopyranoside).

**DPPH and Hydroxyl Radical (·OH) Scavenging Activity** In a 96 micro-well plate, 100 $\mu$L of each sample were added to an ethanol solution of DPPH (60 $\mu$M).[24] After vortexing, the mixture was incubated for 30 min at room temperature and the absorbance was measured at 540 nm. The DPPH radical-scavenging activity was recorded as a percentage (%) compared to the control.[25] The reaction mixture contained 10 mM $FeSO_4 \cdot 7H_2O_2$–ethylenediaminetetraacetic acid (EDTA), 10 mM 2-deoxyribose, and the sample solutions. After incubation at 37°C for 4 h, the reaction was quenched by the addition of 2.8% trichloroacetic acid and 1.0% thiobarbituric acid solution. The solution was heated to reflux for 20 min and then cooled in a water bath. The ·OH scavenging activity was measured at 490 nm.

**Anti-bacterial Activity** *Escherichia coli* and *Staphylococcus aureus* were provided by the Korean Culture Center of Microorganisms (KCCM, Seoul, Korea). Trypticase Soy Agar (TSA) was purchased from BD Difco (NJ, U.S.A.), and disc paper was obtained from Adabantec (Tokyo, Japan). The TSA culture medium contained pancreatic digest of casein (15 g), papaic soybean digest (5 g), NaCl (5 g), and agar (15 g) in distilled water (1 L). Microaerophilic conditions were maintained at 37°C. *Helicobacter pylori*, provided by the Korean Type Culture Collection (KTCC, Daejeon, Korea), was cultured in brucella broth (Difco, NJ, U.S.A.) containing 10% horse serum (Welgene, Daegu, Korea). For testing, *H. pylori* was grown on a medium prepared with (per liter) BD Bactodextrose (1 g), BD Bactoyeast extract (2 g) (Becton, Dickinson and Company [BD], Franklin Lakes, NJ, U.S.A.), sodium chloride (5 g), and sodium bisulfate (0.1 g). Anti-bacterial activity against *S. aureus*, *E. coli*, and *H. pylori* was measured by the disc agar method.[26] Plates of medium were spread with 0.1 mL of culture broth, and 500 $\mu$M solutions of the compounds were pipetted onto sterile filter paper discs (8 mm). Inhibition zones were determined after 24 h at 37°C.

**Cell Culture** AGS cells were maintained in RPMI-1940 medium and RAW264.7 cells were cultured in DMEM containing 100 U·mL$^{-1}$ of penicillin–streptomycin and 10% FBS at 37°C in a 5% $CO_2$ incubator. Cells were sub-cultured weekly with 0.05% trypsin–EDTA in phosphate buffered saline.

**Cell Viability Assay** After confluence had been reached, the cells were plated at a density of $5\times10^4$ cells·well$^{-1}$ into 24-well plates, incubated for 2 h and then treated with LPS (1 $\mu$g·mL$^{-1}$) and IFN-$\gamma$ (10 ng·mL$^{-1}$) for 24 h. After incubation, cell viability was determined using the MTT assay. MTT solution was added to each 24-well plate, the plates were incubated for 4 h at 37°C, and the medium containing MTT was removed. The incorporated formazan crystals in the viable cells were solubilized with DMSO (1 mL) and the absorbance of each well was read at 540 nm.[27]

**Measurement of Nitrite** Nitric oxide (NO) production was assayed by measuring the accumulation of nitrite using a microplate assay method based on the Griess reaction.[28] RAW264.7 cells were seeded in 96-well plates ($5\times10^4$ cells·well$^{-1}$) and LPS (1 $\mu$g·mL$^{-1}$) and IFN-$\gamma$ (10 ng·mL$^{-1}$) were added. After incubating the samples for 24 h, 100 $\mu$L of culture supernatant was allowed to react with 100 $\mu$L of Griess reagent and the mixture was incubated at room temperature for 15 min. The optical density of the samples were measured at 540 nm using a microplate reader.[29]

**Statistical Analysis** Results are expressed as the mean±standard deviation (S.D.). Statistical significance was determined by Duncan's multiple range tests using SAS software (version 6.0; SAS Institute, Cary, NC, U.S.A.). Significance was set at $p<0.05$.

Compound **1**: White amorphous powder, $[\alpha]_D^{27}$ +2.9 ($c$=0.025, MeOH); UV (MeOH): $\lambda_{max}$ 265, 281, and 337 nm (log$\varepsilon$: 3.30, 3.45, and 3.27); IR (KBr): $\nu_{max}$ 3343 and 1072 (hydroxyl groups and the glycosidic linkage) cm$^{-1}$; $^1$H- and $^{13}$C-NMR (500 MHz, pyridine-$d_5$): Table 1.

Compound **2**: White amorphous powder, $[\alpha]_D^{27}$ +75.5 ($c$=0.025, MeOH); UV (MeOH): $\lambda_{max}$ 262 and 289 nm (log$\varepsilon$: 3.20, and 2.60); IR (KBr): $\nu_{max}$ 3339 and 1073 (hydroxyl groups and the glycosidic linkage) cm$^{-1}$; $^1$H- and $^{13}$C-NMR (500 MHz, pyridine-$d_5$): Table 1.

Compound **3**: White amorphous powder, $[\alpha]_D^{27}$ +11.7 ($c$=0.1, MeOH); UV (MeOH): $\lambda_{max}$ 261 and 281 nm (log$\varepsilon$: 3.20 and 3.50); IR (KBr): $\nu_{max}$ 3365 and 1071 (hydroxyl groups and the glycosidic linkage) cm$^{-1}$; $^1$H- and $^{13}$C-NMR (500 MHz, pyridine-$d_5$): Table 1.

Compound **4**: White amorphous powder, $[\alpha]_D^{27}$ +2.4 ($c$=0.025, MeOH); UV (MeOH): $\lambda_{max}$ 243, 281, and 301 nm (log$\varepsilon$: 3.00, 2.60, and 1.90); IR (KBr): $\nu_{max}$ 3341 and 1073 (hydroxyl groups and the glycosidic linkage) cm$^{-1}$; $^1$H- and $^{13}$C-NMR (500 MHz, pyridine-$d_5$): Table 1.

**Acknowledgments** This research was supported by a Grant from Korea Food Research Institute (2012), Republic of Korea and Cooperative Research Program for Agriculture Science & Technology Development (Project No. PJ011582052015), Rural Development Administration, Republic of Korea.

**Conflict of Interest** The authors declare no conflict of interest.

## References

1) Paul M. C., Marc R. B., Gordon M. G., Mark L., Joel M., Jeffrey D. W., "Encyclopedia of Dietary Supplements," Marcel Dekker, New York, 2005, p. 262.
2) Chan C. F., Wu S. H., *Trends Food Sci. Technol.*, **17**, 320 (2006).
3) Yue P. Y., Mak N. K., Cheng Y. K., Leung K. W., Ng T. B., Fan D. T., Yeung H. W., Wong R. N., *Chin. Med.*, **2**, 6–21 (2007).
4) Hofseth L. J., Wargovich M. J., *J. Nutr.*, **137** (Suppl.), 183S–185S

(2007).
5) Chen C. F., Chiou W. F., Zhang J. T., *Acta Pharmacol. Sin.*, **29**, 1103–1108 (2008).
6) Jung C. H., Seog H. M., Choi I. W., Cho H. Y., *Food Chem.*, **92**, 535–540 (2005).
7) Sun B. S., Gu L. J., Fang Z. M., Wang C. Y., Wang Z., Lee M. R., Li Z., Li J. J., Sung C. K., *J. Pharm. Biomed. Anal.*, **50**, 15–22 (2009).
8) Bae E. A., Han M. J., Baek N. I., Kim D. H., *Arch. Pharm. Res.*, **24**, 297–299 (2001).
9) Zhu J. H., Takeshita T., Kitagawa I., Morimoto J., *Cancer Res.*, **55**, 1221–1223 (1995).
10) Shibata S., Tanaka O., Nagai M., Ishii T., *Chem. Pharm. Bull.*, **11**, 762–765 (1963).
11) Shibata S., Ando T., Tanaka O., Meguro Y., Sôma K., Iida Y., *Yakugaku Zasshi*, **85**, 753–755 (1965).
12) Shibata S., Tanaka O., Soma K., Ando T., Iida Y., Nakamura H., *Tetrahedron Lett.*, **42**, 207–213 (1965).
13) Wang J. H., Li W., Sha Y., Tezuka Y., Kadota S., Li X., *J. Asian Nat. Prod. Res.*, **3**, 123–130 (2001).
14) Popovich D. G., Kitts D. D., *Phytochemistry*, **65**, 337–344 (2004).
15) Hong H. D., Choi S. Y., Kim Y. C., Lee Y. C., Cho C. W., *J. Ginseng Res.*, **33**, 8–12 (2009).
16) Sun J., Hu S., Song X., *Vaccine*, **25**, 1114–1120 (2007).
17) Wang J. R., Yamasaki Y., Tanaka T., Kouno I., Jiang Z. H., *Molecules*, **14**, 2087–2094 (2009).
18) Iwamoto M., Fujioka T., Okabe H., Mihashi K., Yamauchi T., *Chem. Pharm. Bull.*, **35**, 553–561 (1987).
19) Tung N. H., Cho K., Kim J. A., Song G. Y., Kim Y. H., *Bull. Korean Chem. Soc.*, **31**, 1381–1384 (2010).
20) Baek N. I., Kim J. M., Pakr J. H., Ryu J. H., Kim D. S., Lee Y. H., Park J. D., Kim S. I., *Arch. Pharm. Res.*, **20**, 280–282 (1997).
21) Chen F., Luo J., Kong L., *J. Liq. Chromatogr. R. T*, **35**, 912–923 (2012).
22) Ping Z., Liu Y. Q., Yang C. R., *Phytochemistry*, **41**, 1419–1422 (1996).
23) Kim D. S., Chang Y. J., Zedk U., Zhao P., Liu Y. Q., Yang C. R., *Phytochemistry*, **40**, 1493–1497 (1995).
24) Hatano T., Edamatsu R., Hiramatsu M., Mori A., Fujita Y., Yasuhara T., Yoshida T., Okuda T., *Chem. Pharm. Bull.*, **37**, 2016–2021 (1989).
25) Chung S. K., Osawa T., Kawakishi S., *Biosci. Biotechnol. Biochem.*, **61**, 118–123 (1997).
26) Davidson P. M., Parish M. E., *Food Technol.*, **43**, 148–155 (1989).
27) Mosmann T., *J. Immunol. Methods*, **65**, 55–63 (1983).
28) Sreejayan, Rao M. N., *J. Pharm. Pharmacol.*, **49**, 105–107 (1997).
29) Chiou W. F., Sung Y. J., Liao J. F., Shum A. Y., Chen F., *J. Natl. Proc.*, **60**, 708–711 (1997).